High-Throughput Mass-Spectrometry Monitoring for Multisubstrate Enzymes: Determining the Kinetic Parameters and Catalytic Activities of Glycosyltransferases

Min Yang,[a] Melissa Brazier,[b] Robert Edwards,[b] and Benjamin G. Davis*[a]

A novel high-throughput screening (HTS) method with electrospray time-of-flight (ESI-TOF) mass spectrometry allows i) rapid and broad screening of multisubstrate enzyme catalytic activity towards a range of donor and acceptor substrates; ii) determination of full multisubstrate kinetic parameters and the binding order of substrates. Two representative glycosyltransferases (GTs, one common, one recently isolated, one O*-glycosyltransferase (O-GT), one* N*-glycosyltransferase (N-GT)) have been used to validate this system: the widely used bovine β-1,4-galactosyltransferase (EC 2.4.1.22), and the recently isolated* Arabidopsis thaliana *GT UGT72B1 (EC 2.4.1.-). The GAR (green/amber/red) broad-substrate-specificity screen, which is based on the mass ion abundance of product, provides a fast, high-throughput method for finding potential donors and acceptors from substrate libraries. This was evaluated by using six natural and non-natural donors (α-UDP-D-Glucose (UDPGlc), α-UDP-*N*-Acetyl-D-glucosamine (UDPGlcNAc), α-UDP-D-5-thioglucose (UDP5SGlc), α-GDP-L-fucose (GDPFuc), α-GDP-D-mannose (GDPMan), α,β-UDP-D-mannose (UDPMan)) and 32 broad-ranging acceptors (sugars, plant hormones, antibiotics, flavonoids, coumarins, phenylpropanoids and benzoic acids). By using the fast-equilibrium assumption, K_M, k_{cat} and K_{IA} were determined for representative substrates, and these values were used to determine substrate binding orders. These screening methods applied to the two very different enzymes revealed some unusual substrate specificities, thus highlighting the utility of broad-ranging substrate screening. For UGT72B1, it was shown that the donor specificity is determined largely by the nucleotide moiety. The method is therefore capable of identifying GT enzymes with usefully broad carbohydrate-transfer ability.*

Introduction

Leloir-type glycosyltransferases (GTs or GlyTs) catalyse the transfer of sugar glycosyl moieties from an electrophilic mono- or diphosphate sugar nucleotide to a nucleophilic (typically O or N) glycosyl acceptor.[1] GTs may be divided into 66 families,[2] which can be further subdivided according to catalytic mechanism into inverting and retaining glycosyltransferases. As enzymes using two substrates and producing two products, their kinetic behaviours are different to those analysed through single-substrate and pseudo-single-substrate approximations (Michaelis–Menten).

To date various assays have been used to study the kinetics of glycosyltransferases,[3] including the use of radiochemicals,[4,5] immunological methods,[4,6,7] spectrophotometric assays,[8] chromatography[9] and some examples of mass spectrometry.[10,11] Mass spectrometry (MS) offers a potentially fast, robust and sensitive method, especially for those reactions that otherwise cannot be easily monitored.[12] In particular, it can simultaneously determine both substrate depletion and product accumulation to widen the source of potentially useful data.

Three publications have recently highlighted the potential for investigating enzyme kinetics by using ESI-MS.[10,11,13] However, all require a high level of manual experimental manipulation, which is not well suited to high-throughput screening (HTS) methods. Here we describe a novel automated method that has allowed rapid and broad assessment of two representative glycosyltransferases.[14]

A plant glycosyltransferase from *Arabidopsis thaliana* UGT72B1 (EC 2.4.1.-)[15] and a mammalian (bovine) β-1,4-galactosyltransferase (β-GalT; 2.4.1.22)[16] were selected to test our method. Ideally, for comparative purposes, parameters have been previously established by different conventional methods for both of these enzymes. β-GalT is one of the most widely used enzymes for the synthesis of glycosidic bonds and is commercially available. It transfers the galactosyl moiety from α-UDP-D-galactose (UDPGal) to an acceptor with inversion of anomeric configuration to form β-*O*-galactosides. In contrast to β-GalT, UGT72B1 from *Arabidopsis* is an *N*-glycosyltransferase. It is a family 1 GT;[2] the excitingly wide-ranging role of these

[a] *Dr. M. Yang, Dr. B. G. Davis*
Department of Chemistry, University of Oxford
Chemistry Research Laboratory
Mansfield Road, Oxford, OX1 3TA (UK)
Fax: (+44) 1865-275-674
E-mail: ben.davis@chem.ox.ac.uk

[b] *Dr. M. Brazier, Prof. R. Edwards*
School of Biological and Biomedical Sciences, University of Durham
South Road, Durham, DH1 3LE (UK)

Supporting information for this article is available on the WWW under http://www.chembiochem.org or from the author: 21 page pdf file of additional kinetic analysis and hyperlinked GAR screen results.

  DOI: 10.1002/cbic.200400100 *ChemBioChem* **2005**, *6*, 346 – 357

enzymes in plants has recently been highlighted,[17] but is largely unexplored. Only recently isolated,[15] UGT72B1 appears to detoxify certain pollutants, such as 3,4-dichloroaniline (3,4-DCA), by transferring the glucose moiety from UDPGlc to form *N*-glycosides.

Results and Discussion

Method development

To accurately quantify concentrations and concentration changes, we developed a method that relies upon an internal standard. While potentially more convenient, experiments to measure component concentrations simply from their absolute total ion count (TIC) without internal standard but with external calibration essentially failed. Although some broad trends in TIC that corresponded to concentration were observed, the data obtained displayed a low response correlation ($R^2 = 0.58$).

However, pleasingly, similar experiments with a fixed concentration of an internal standard (GDP) gave an excellent linear response ($R^2 \geq 0.97$) and was subsequently selected as the calibration method of choice. Ideally, internal standards should be similar to the substrates of interest to ensure similar ionisation response in MS.[11] We chose GDP because of the consistent use of nucleotide donors in our chosen GlyT reactions.

Introduction of an internal standard directly into a given reaction system, although potentially convenient, might also cause inhibition. This is especially pertinent to GTs, for which feedback inhibition by nucleotide diphosphates (NDPs) is prevalent. Furthermore, a given standard might not be stable under reaction conditions. Indeed, during initial experiments, problems with use of "in-reaction" standards were highlighted by observed GDP decomposition with certain benzoic acid acceptors plus, in many cases, high feedback inhibition of the GT enzymes. Previous methods[10,11] have added internal standards after manual aliquot removal and quenching work-up procedures; a solution that is time consuming and therefore not amenable to HTS.

Thus, to avoid potential interference with the enzyme assay, the GDP internal standard was introduced into the mass-spectrometer injection loop by using an HPLC autosampler immediately prior (within 0.3 min) to the injection of the reaction mixture to be tested. Suitable adjustment of the injection loop and sample tubing between HPLC and MS ensured that a consistent GDP standard signal appeared at ~0.7 min and lasted during the reaction mixture (donor, acceptor, products) signals, which appeared at ~1.2 min onwards (Figure 1).

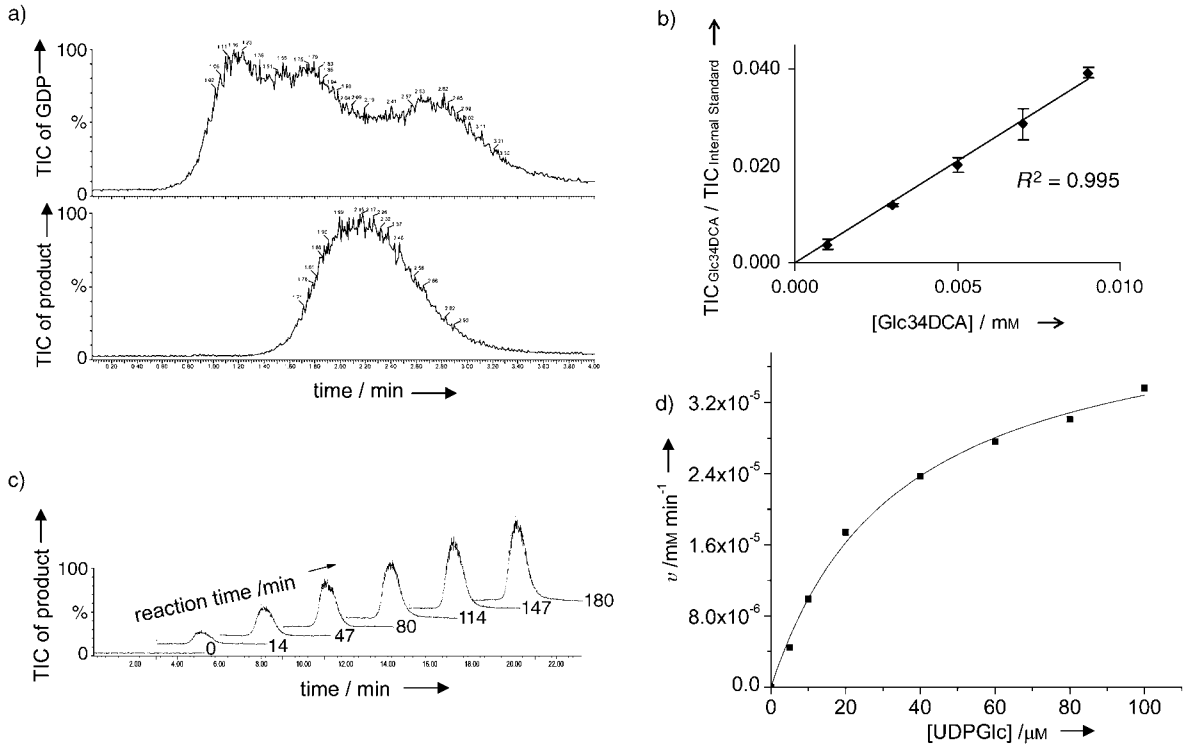

Figure 1. *a) Typical TIC time course of GDP and product obtained during the monitoring of UGT72B1 activity. Adjustment of concentration and conditions ensured a "blanket" background GDP standard ion count (upper spectrum, y scale shows % of maximum ion count, TIC = 3.1 × 10⁴) covering the time period of the product ion count without needing to introduce the standard to sample solution ("pseudospiking"). While some ion suppression of GDP signal (< 10%) is observed at high concentrations of product, at the low concentrations used for initial rate kinetic methods there is little or no effect. b) Good calibration ($R^2 = 0.995$) of TIC to concentration is seen in calibration curves, illustrated here for glucosylated 3,4-dichloroaniline (Glc34DCA). c) Time-course TIC measurements of products therefore allow good determination of concentration time courses from which initial rates may be determined, illustrated here for formation of Glc34DCA by using UGT72B1. d) Under pseudo-single-substrate conditions, this in turn allows the determination of Michaelis–Menten curves, illustrated here for formation of Glc34DCA by using UGT72B1.*

Hence, the two solutions, standard and sample, were monitored through near-simultaneous analysis ("pseudosimultaneous spiking"), thus allowing internal calibration ($R^2 \geq 0.97$) in a manner suitable for high-throughput screening, without any potential effect (inhibition, etc.) of the internal standard on the reaction or on the standard itself.

Additional parameters affecting the MS quantification were also investigated. The signal/background noise (S/N) ratio can be adversely affected during monitoring due to buffer ionisation at a higher level than that of the reactants or product due to their relative concentrations in the assay. Bufferless reaction solutions are thus ideal in MS. In our assays, while such solutions improved S/N they proved impractical. For example, in the absence of Tris buffer and the resulting nonoptimal, unstable reaction pH, the turnover of enzyme UGT72B1 was extremely slow and variable. A variety of buffers and corresponding elution-solvent systems were evaluated—notably MeCN/H_2O/Et_3N, 35:65:0.2;[11] $NH_4OAc/NH_3/H_2O$, 1 mM, pH 8.0 and MeCN/H_2O, 1:1—from which Tris with MeCN/H_2O 1:1 proved the best solvent for all systems. The effect of buffer was further minimised by the use of a baffled, "Z" channel mass spectrometer.[18] GT enzymes such as β-GalT may require metal ion cofactors (Mn^{2+}), which can also interfere with MS analysis. To solve this third experimental problem, the concentrations of cofactor metal salts were minimised to levels that supported optimal enzyme activity yet improved S/N. It should be noted that, in many GT buffer systems,[16] vastly excessive cofactor concentrations are employed that are, in our experience, unnecessarily high and beyond those needed for optimal rate. Finally, because the ionisation of certain component reactants/products (UDPGlc salt; sugars) is typically very strong, a very effective signal is obtained. Together, the use and optimisation of these four parameters—pseudosimultaneous spiking, correct buffer pK_a with corresponding elution solvent, Z-channel and low cofactor ion concentration—created a robust and powerful analytical HTS enzyme-monitoring system.

Calibration and data acquisition

In all the reactions studied, five ions were monitored, where possible, in order to obtain the maximum possible information on the progress of the reaction. The ions monitored (ESI^-) were the donor $[M-H^+]^-$, acceptor $[M-H^+]^-$ and/or $[M+{}^{35}Cl^-]^-$, NDP product $[NDP\text{-}H^+]^-$, glycoside product $[M+{}^{35}Cl^-]^-$ and internal standard $[GDP\text{-}H^+]^-$. The total ion counts of each peak were then integrated, and the absolute concentration of each compound was obtained from standard curves after normalising the ionisation efficiencies for each reaction with respect to the internal standard GDP.

Standard curves were constructed for each component at concentrations around those found under the initial reaction conditions needed for initial-rate-method measurements. Thus, concentrations of donor and acceptor were typically varied from 10–100 μM at 20 μM intervals, while the products (NDP and glycosides) were typically determined at one tenth of the donor concentrations. In each case, the concentration of GDP (internal standard) was fixed at 100 μM (administered through "pseudospiking", vide supra), and the buffer composition was as used in actual reactions. Finally, the TICs for each ion derived from the components of known concentration were integrated. For each compound, the integral of the TIC for a given concentration was then divided by the integral of the TIC of GDP. All the ratios of the concentrations thus obtained were plotted against actual values to give standard plots that in all cases gave excellent linear correlations ($R^2 \geq 0.97$).

For reaction monitoring, donor and acceptor consumption and product formation, as judged by their TIC integrated values, were monitored as a function of time. To allow full determination of the kinetic parameters, one substrate was held at a fixed concentration while the other was varied before the roles were reversed. Later determinations and analyses then allowed uncurtailed variation of either concentration parameter through the use of surface correlation regression analysis (vide infra). Typically each analysis required ~6 min for completion, and, for full parameter evaluation, typically ~80 such injection runs were required, thus highlighting the need for an automated, high-throughput process. In the absence of HTS, only partial parameter determination has been practicable in previous studies.[10,11] In addition, the limited stability of some GT enzymes provides another important reason for rapid throughput.

Kinetic analysis

The Michaelis–Menten steady-state equation[19,20] can be used in single-substrate or pseudo-single-substrate situations but cannot be directly applied to glycosyltransferase enzymes that use two substrates and generate two products. In many studies,[10,11,21] a saturated concentration of one substrate has been used to reduce the kinetic analysis of glycosyltransferases to a pseudo-single-substrate reaction. However, the data generated under these circumstances do not reflect the general properties of the enzyme and, indeed, can only be applied to the analysis of such atypical saturation conditions. These analyses are therefore of limited utility.

For two substrate reactions as catalysed by GTs, steady-state assumptions may be reliably applied to multisubstrate enzyme reactions.[22] King–Altman analysis[23] allows the reaction equation of an "ordered bi bi" reaction, Cleland nomenclature,[24] to be analysed (Scheme 1).[25]

$$E + A \underset{k_{-1}}{\overset{k_1}{\rightleftharpoons}} EA + B \underset{k_{-2}}{\overset{k_2}{\rightleftharpoons}} (EAB \rightleftharpoons EPQ) \underset{k_{-3}}{\overset{k_3}{\rightleftharpoons}} EQ + P \underset{k_{-4}}{\overset{k_4}{\rightleftharpoons}} E + Q$$

Scheme 1. *Ordered bi bi enzyme mechanism. A, B: substrates, E: enzyme, P, Q: products.*

For initial-rate studies, such as those described here, this may be simplified with the assumption [P] = [Q] = 0 to give:

$$\theta = \frac{V_{max}[A][B]}{K_{IA}K_B + K_B[A] + K_A[B] + [A][B]} \quad (1)$$

K_A and K_B are the K_Ms for each substrate, and K_{IA} is the dissociation constant for the EA complex. With a fixed concentration of one substrate, for example, A, a Lineweaver–Burk plot analysis, for example, $1/\vartheta$ versus 1/[B], can be performed.

$$\frac{1}{\theta} = \frac{K_B}{V_{max}}\left(1 + \frac{K_{IA}}{[A]}\right)\frac{1}{[B]} + \frac{K_A + [A]}{V_{max}[A]} \quad (2)$$

Since, if the concentrations of A are greatly in excess of K_{IA}, the variation in slopes of $1/\vartheta$ versus 1/[B] at different [A]s is non-responsive, the concentrations of both substrates in the kinetic experiments with the GTs were kept low (20–100 μM).

For random bi bi reactions (Scheme 2), King–Altmann analysis coupled with computational assessment[26] allows Equation (3) to be derived.

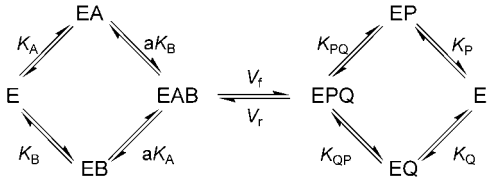

Scheme 2. *Random bi bi enzyme mechanism.*

$$\theta = \frac{VK_a[A][B] + K_b[A]^2[B] + [A][B]^2}{K_c + K_d[A] + K_e[B] + K_f[A]^2 + K_g[B]^2 + K_h[A][B] + K_i[A]^2[B] + [A][B]^2} \quad (3)$$

The definitions of the various kinetic constants, K_a–K_i, differ from those in the ordered mechanism.[27] The random bi bi kinetic Equation (3) maybe simplified with the assumption that all steps other than the central conversion of EAB⇄EPQ are in rapid equilibrium. The equation for this system (rapid-equilibrium random bi bi) can be obtained from the associated Equation (3) by eliminating all the terms that contain either of the rate constants for the central EAB-to-EPQ step. The resulting rate equation is then identical in form to the ordered bi bi but without terms in [A][P], [B][Q], [A][B][P] and [B][P][Q] in the denominator. This conveniently leads to the same general Equation (1). The similar form proves ideal for parallel data analysis, although it should be noted that the interpretation of resulting constants crucially differs. Definitions for the kinetic constants for random bi bi are the same as for ordered bi bi except that K_{IB} = constant/coef B and K_{IP} = constant/coef P.[22]

Although there are several examples of ordered bi bi mechanistic studies, there are only a relatively limited number of examples for the GTs.[28–36] The general strategy for studying multisubstrate enzyme kinetics is to initially determine mechanism (ordered vs. random). In our method, application of the rapid-equilibrium assumption (REA)[25] advantageously allowed Equation (3) to be simplified to Equation (1). The following kinetic parameters were obtained from nonlinear regression: V_{max} (k_{cat}), K_A, K_B, K_{IA} and K_{IB}. In all cases, two parallel regressions reversing the substrate identities (i.e. A = donor cf. A = acceptor) were compared, with consistent values for K_M for each substrate being obtained regardless of assigned identity.

In each case, the K_B/K_A or K_{IB}/K_{IA} ratio was used to determine the enzyme mechanism, K_M indicating the binding affinity of an enzyme for its substrate and K_{IB} and K_{IA} being the dissociation constants for enzyme–substrate complexes. Theoretical support for this assumption can be deduced from Equation (3). For an ordered bi bi mechanism:

$$\frac{K_B}{K_A} = k_1k_4\frac{k_{-2} + k_3}{k_2k_3k_4} = \frac{k_1}{k_2}\left[1 + \frac{k_{-2}}{k_3}\right] \quad (4)$$

$$\frac{K_{IB}}{K_{IA}} = \frac{k_{-3}k_{-4}(k_{-1} + k_{-2})/(k_2k_{-3}k_{-4})}{k_{-1}/k_1} = \frac{k_1}{k_2}\left[1 + \frac{k_{-2}}{k_{-1}}\right] \quad (5)$$

while for a rapid-equilibrium random bi bi mechanism:

$$\frac{K_B}{K_A} = k_1k_4\frac{k_{-2} + k_3}{k_2k_3k_4} = \frac{k_1}{k_2}\left[1 + \frac{k_{-2}}{k_3}\right] \quad (6)$$

$$\frac{K_{IB}}{K_{IA}} = \frac{k_{-1}k_4(k_{-2} + k_3)/k_2k_3k_4}{k_{-1}/k_1} = \frac{k_1}{k_2}\left[1 + \frac{k_{-2}}{k_3}\right] \quad (7)$$

in which $(k_1/k_2) \propto (K_B/K_A)$ and (K_{IB}/K_{IA}).

Thus, if $k_{-2} \ll k_3$ then

$$\frac{K_B}{K_A} = \frac{k_1}{k_2}\left[1 + \frac{k_{-2}}{k_3}\right] \cong \frac{k_1}{k_2} \quad (8)$$

A literature survey reveals that the K_B/K_A ratio is a strongly correlated guide to either ordered or random bi bi mechanism: ordered bi bi reactions display K_B/K_A in the range = 7.4–485,[35–43] while random bi bi mechanism display K_B/K_A = 1.1–7.5.[44–49] We would therefore suggest that a threshold of $K_B/K_A > 10$ is suitable for defining an ordered bi bi reaction.

Bovine β-1,4-galactosyltransferase (β-GalT)

β-GalT[50–53] catalyses the transfer of the galactosyl moiety of UDPGal to an acceptor to form β-galactoside with inversion of anomeric configuration. Despite the availability of β-GalT, the determination of its kinetic parameters has been limited to only a handful of donor–acceptor pairs.[16,51–53] For initial comparison of the results obtained for the kinetic characterisation of β-GalT by the HTS MS method with the more-traditional determination of activity by using fluorescence,[16] the methylumbelliferyl (MU) glycoside of *N*-acetylglucosamine (MUGlcNAc) was used as acceptor in a reaction catalysed by β-GalT with UDPGal (Scheme 3). The reaction was monitored as described above by using the TIC time course with GDP as the "pseudo-spike" internal standard. Both nonlinear regression and linear (Lineweaver–Burk)[54] analyses gave similar absolute values, but the former gave better precision. The kinetic parameters determined by using MS are shown in Table 1 and compared with those determined in earlier studies[16] in parentheses.

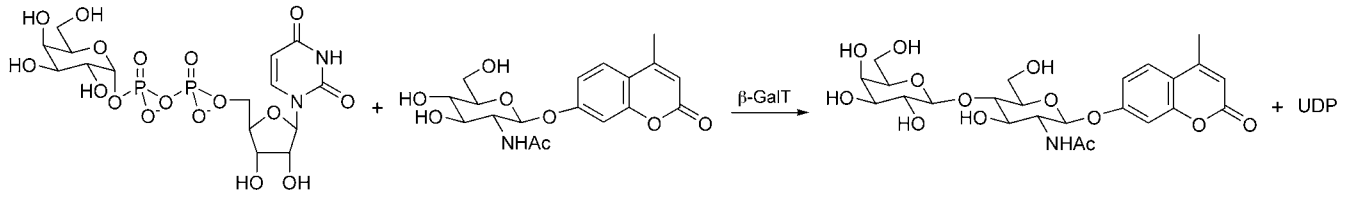

Scheme 3. *Reaction of UDPGal with MUGlcNAc catalysed by β-GalT.*

Table 1. *Kinetic parameters for β-GalT with MUGlcNAc and UDPGal as substrates.*[a]

Equation	UDPGal as A[b] $Y=\frac{1}{(P1/A\times B)/(P2\times P4+P3\times B+P4/A+B/A)}$	MUGlcNAc as A[b] $Y=\frac{1}{(P1\times A/B)/(P2\times P4+P3/B+P4\times A+A/B)}$
V_{max} [min mM^{-1}]	$8\times10^{-5}\pm3.9\times10^{-6}$	$8\times10^{-5}\pm3.9\times10^{-6}$
$K_{I(UDPGal)}$ [μM]	19 ± 2 (n.d.[c])	–
$K_{I(MUGlcNAc)}$ [μM]	–	5 ± 0.2 (n.d.[c])
$K_{M(UDPGal)}$ [μM]	76 ± 4 (115.3[c])	76 ± 4
$K_{M(MUGlcNAc)}$ [μM]	19 ± 2 (35.9[c])	19 ± 2
k_{cat} [s^{-1}]	0.0061	
$k_{cat}/K_{M\ (UDPGal)}$ [M^{-1}s^{-1}]	80	
$k_{cat}/K_{M\ (MUGlcNAc)}$ [M^{-1}s^{-1}]	316	

[a] $R^2=0.998$ at 95% confidence. [b] P1–P4 are kinetic parameters: P1 = V_{max}, P2 = K_{IA}, P3 = K_A and P4 = K_B. [c] Taken from Kanie et al.,[16] n.d. indicates not determined in this earlier study.

A fair correlation between the data obtained and those reported previously[16] was observed (Table 1). The ratio of K_B/K_A ~4 for UDPGal and MUGlcNAc indicated that, although MUGlcNAc was slightly more favoured for substrate binding, the reaction mechanism was random bi-bi.

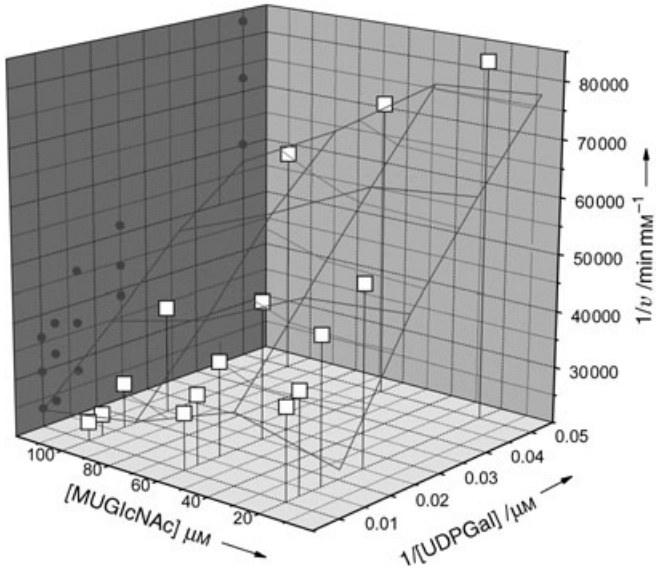

Figure 2. *3D plot of β-GalT kinetics. This figure indicates all Lineweaver–Burk plots as the two concentration parameters [MUGlcNAc] and [UDPGal] vary. The projections of each point onto the ZX plane (left) are also shown (●). Full kinetic parameters were determined by nonlinear regression analysis that allowed simultaneous fitting of the data to result in the 3D surface shown.*

As well as providing a method for detailed kinetic analysis, the HTS also allows ready comparison of enzyme activities. For example, comparison of two bovine β-GalT enzyme sources, one purified directly from bovine milk (β-GalT-milk) the other from a recombinant source (*Spedoptera frugiperda*, rβ-GalT) was conducted by using MUGlcNAc as an acceptor. Under identical reaction conditions, equal enzyme concentrations at a substrate concentration of 0.5 mM, an initial rate for rβ-GalT that was 2.5-fold higher than that for β-GalT-milk was observed (Figure 2).

UGT72B1

Recombinant protein rUGT72B1 was generated by using IPTG-induced expression of a pET-11d vector construct with BL21-DE3 Rosetta *E. coli* as host.[15] The soluble 50 kDa polypeptide was purified by using Sepharose blue (affinity) column chromatography, with UDPGlc as eluent, followed by dialysis. SDS-PAGE (Figure 3) showed the enrichment of the recombinant GT (expected molecular mass 52928 Da). Overall, the purity of the preparation was assessed to be ≥95%.

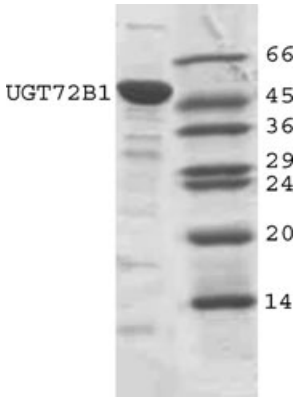

Figure 3. *SDS-PAGE of UGT72B1. Left-hand lane: purified UGT72B1, right-hand lane: SDS7 molecular mass (kDa) standards.*

The activity of UGT72B1 towards UDPGlc and 3,4-DCA was examined by using our novel HTS method and compared with the previous radiochemical-based assay.[15] The product peak at 358 with its characteristic isotope pattern (Figure 4) was used as the primary monitor for this reaction.

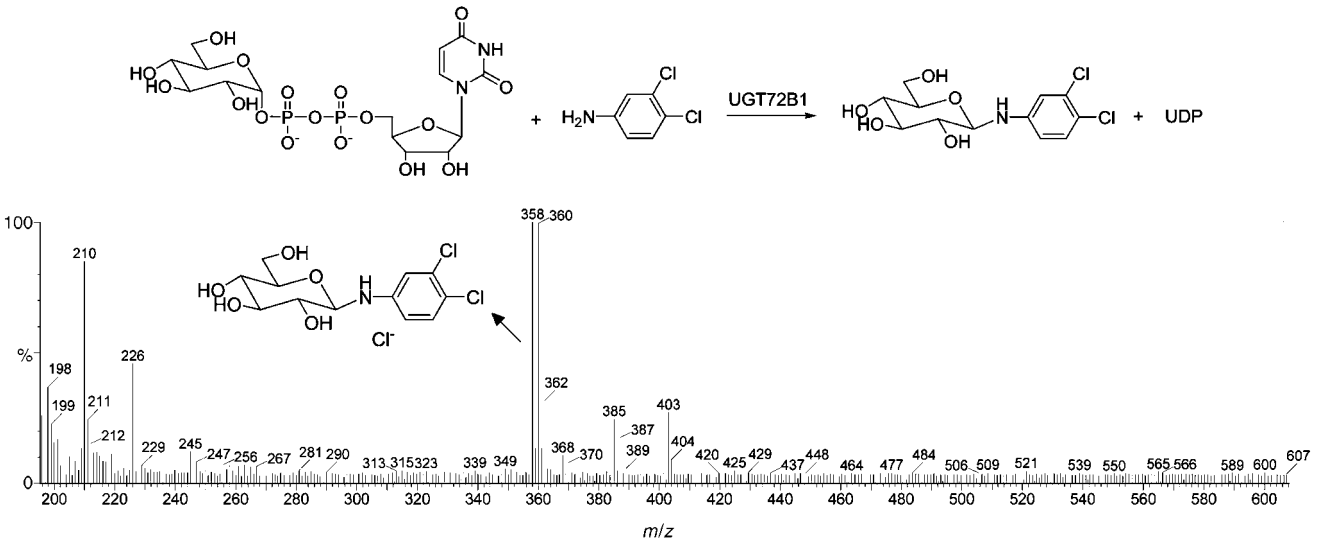

Figure 4. *Mass spectrum of the reaction of UDPGlc with 3,4-DCA catalysed by UGT72B1. Peaks at 358, 360 and 362 are for the target product DCA-Glc as $[M+Cl^-]^-$ ions, with expected 100:96:32 isotope distribution.*

Reactions were monitored by using TIC in the linear initial-rate region over ~90–200 min, and kinetic parameters were determined by using both double reciprocal analysis and non-linear regression with the two contrasting hypotheses: UDPGlc is A, c.f. UDPGlc is B, as for β-GalT (Figure 5 and Table 2).

Pleasingly, the results correlated relatively well with similar data determined by Loutre et al.[15] using more classical radiochemical methods. In addition, based on the approximately twofold differences in K_M towards DCA and UDPGlc, it was concluded that UGT72B1-catalysed glucosylation of DCA does not proceed by an ordered mechanism.

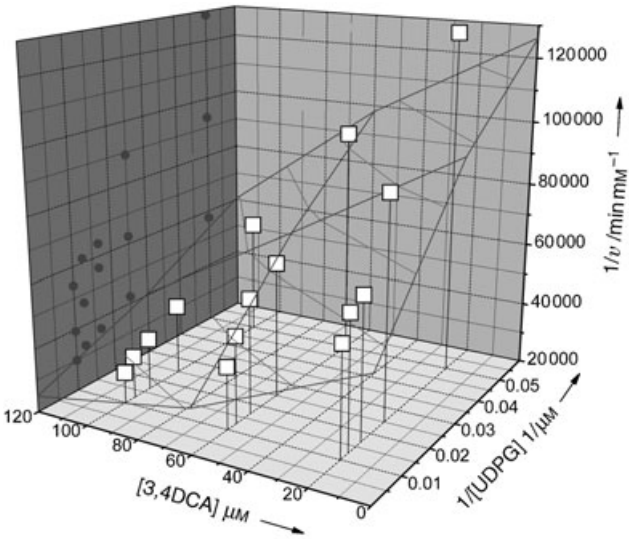

Figure 5. *3D plots of UGT72B1 kinetics. This figure indicates all Lineweaver–Burk plots as the two concentration parameters [3,4DCA] and [UDPGlc] vary. The projections of each point onto the ZX plane (left) are also shown (●). Full kinetic parameters were determined by nonlinear regression analysis that allowed simultaneous fitting of the data to result in the 3D surface shown.*

Broad screening (GAR) for the potential acceptors and donors

Having achieved reasonable agreement with published kinetic parameters, which had been obtained by alternative methods, for these two very different enzymes, the MS method was then applied as a broad screen for GT activity designed to rapidly identify potential acceptors and donors. To investigate the full extent of the substrate specificity of the recently isolated GT UGT72B1, a high-throughput library-screening format was used to assess its ability to transfer different representative donors to a variety of potential acceptors by using a "green-amber-red" (GAR) qualitative notation based on the relative endpoint signal-to-noise ratio of the expected product TIC peaks [Green S/N > 10, Amber S/N = 1–10]. A 32 compound acceptor library (Scheme 4) and a six compound donor library (Scheme 5) were used. The general strategy

Table 2. *Kinetic parameters for UGT72B1 with DCA and UDPGlc as substrates.[a]*

Equation	UDPGlc as A[b] $Y=\frac{1}{(P1/A\times B)/(P2\times P4+P3\times B+P4/A+B/A)}$		3,4-DCA as A[b] $Y=\frac{1}{(P1\times A/B)/(P2\times P4+P3/B+P4\times A+A/B)}$
V_{max} [min mM^{-1}]	$4\times10^{-5}\pm4.67\times10^{-6}$		$4\times10^{-5}\pm4.67\times10^{-6}$
$K_{I(UDPGlc)}$ [μM]	97 ± 32 (n.d.[c])		–
$K_{I(34DCA)}$ [μM]	–		42 ± 2.5 (n.d.[c])
$K_{M(UDPGlc)}$ [μM]	25 ± 3 (4.6 ± 2.3[c])		11 ± 4.7
$K_{M(34DCA)}$ [μM]	11 ± 4.7 (22.3 ± 6.8[c])		25 ± 3
k_{cat} [s^{-1}]		0.106	
$k_{cat}/K_{M\ (UDPGlc)}$ [M^{-1}s^{-1}]		4182	
$k_{cat}/K_{M\ (34DCA)}$ [M^{-1}s^{-1}]		9414	

[a] $R^2=0.998$ at 95% confidence. [b] P1–P4 are kinetic parameters: P1 = V_{max}, P2 = K_{IA}, P3 = K_A and P4 = K_B. [c] Taken from Loutre et al.,[15] n.d. indicates not determined in this earlier study.

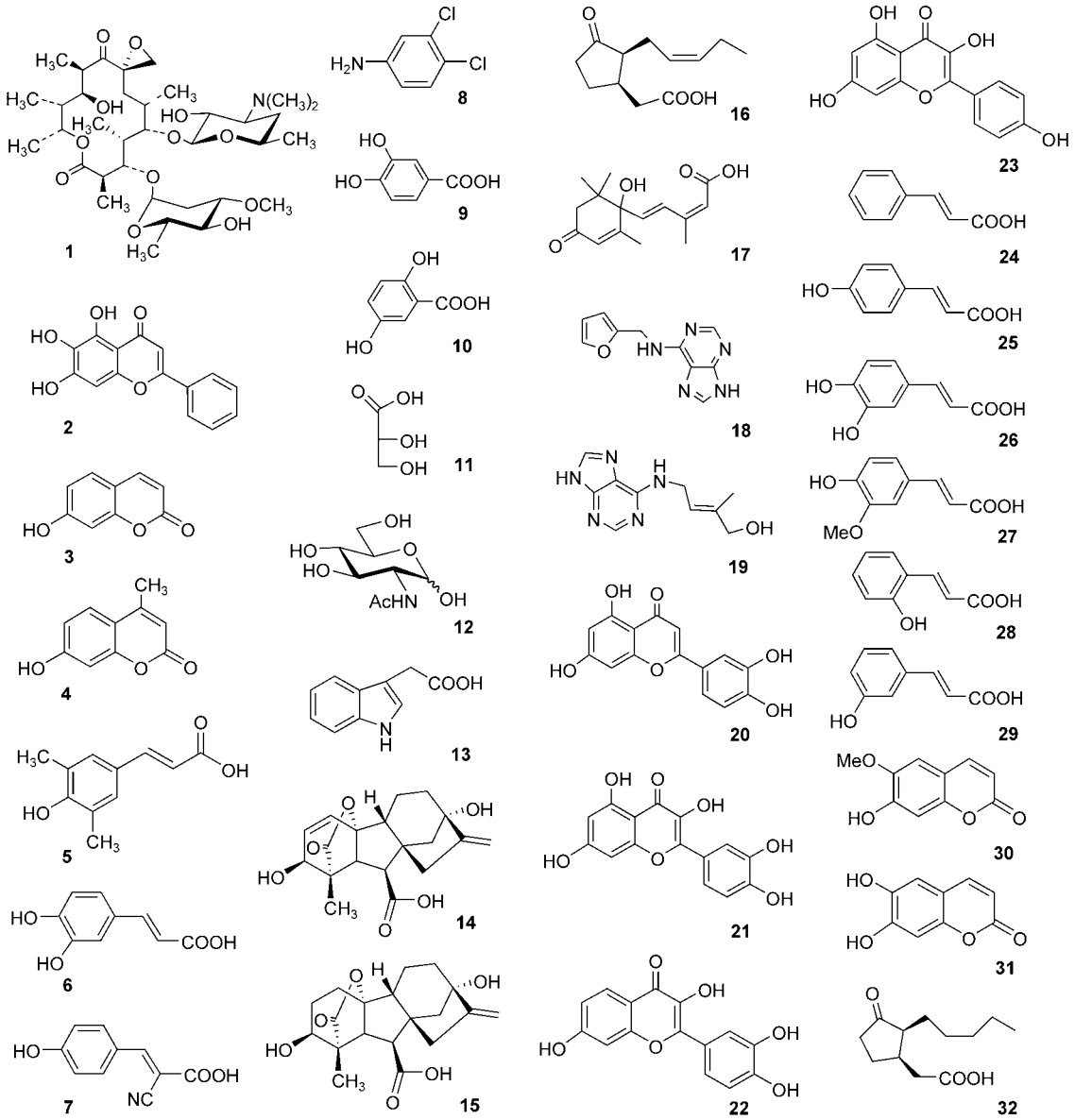

Scheme 4. *Acceptor probe library.*

of this GAR method was to firstly screen known donors against the broad acceptor library, and then secondly use the acceptors identified in this first screen against the wider six-membered sugar donor library. Thus, UDPGlc was first employed as the known donor for UGT72B1.

The qualitative results of screening UGT72B1 with the acceptor library by using UDPGlc are shown in Figure 6. In addition to the known acceptor 3,4-dichloroaniline (**8**), coumarin and benzoic acid analogues, (**3**, **4**, **9**, **10**, **30** and **31**) also served as good acceptors, while structurally similar flavonoids were, intriguingly, not substrates. This subtlety in specificity illustrates that even this rapid screen allows some form of rudimentary substrate-specificity map to be elucidated. A similar GAR broad acceptor-screening experiment was conducted for β-GalT by using the preferred donor UDPGal. These acceptors (Scheme 4) are atypical for β-GalT, yet **3**, **12** and **30** appeared as novel acceptors (GAR plate not shown).

Next, by using the acceptors identified above as probes, novel potential donors (Scheme 5) were identified for UGT72B1. Non-natural substrates, UDP-mannose (UDP-Man) and α,β-UDP-5-thio-glucose (α,β-UDP5SGlc) were synthesised according to Uchiyama and Hindsgaul's method (Scheme 6).[55] To verify activities towards UDP5SGlc, pure anomer α-UDP5SGlc was also obtained by an alternative procedure.[56] Briefly, α,β-5-thioglucose was first fully acetylated and then converted into the corresponding glycosyl bromide. This bromide was coupled with silver dibenzylphosphate, and pure α or β product was separated by column chromatography. For each anomer, hydrogenolytic deprotection gave pure α (α-5SG1P) or β-5-thio-D-glucose-1-phosphate, accordingly. α-5SG1P was then treated with UTP and UDP-glucose pyrophosphorylase to give pure α-UDP5SGlc.[56] Full synthetic details will be published in due course.

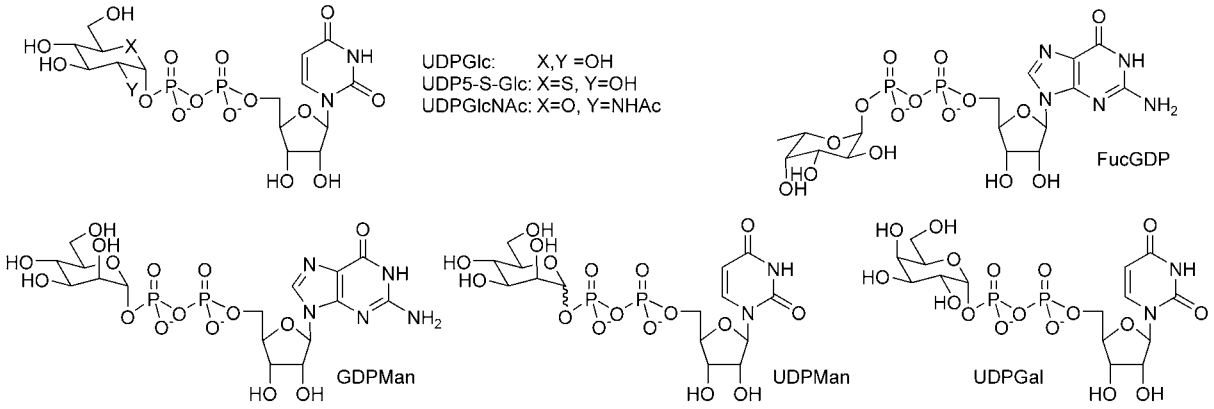

Scheme 5. *Structures of the donors in the library.*

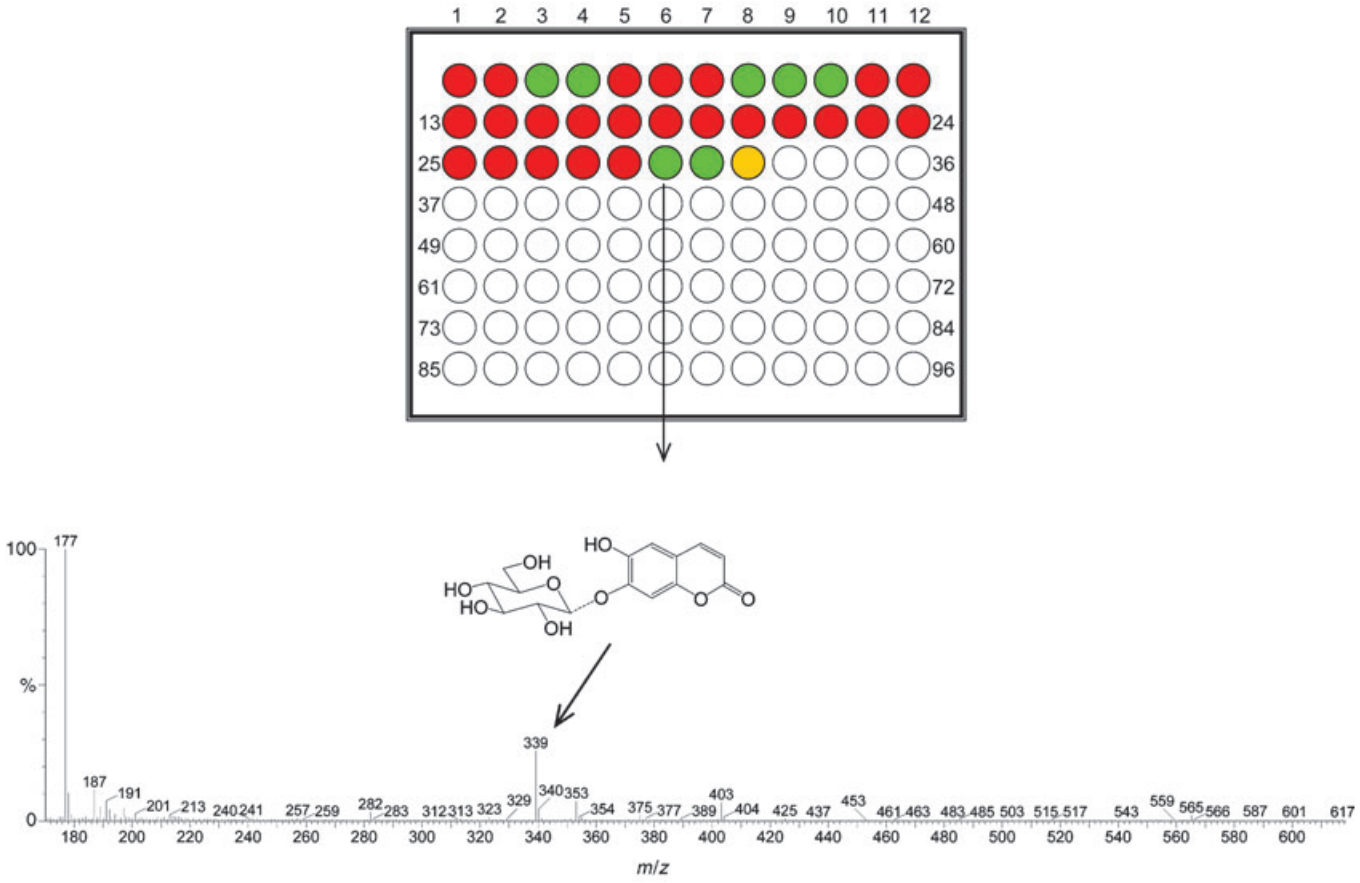

Figure 6. *Mass spectroscopic screening for the conjugating activity of UGT72B1 towards a series of acceptor substrates (Scheme 4) with UDPGlc. The GAR (green-amber-red) results reveal acceptors when using UDPGlc as a donor. The "green-amber-red" qualitative screen is based on the relative TIC signal-to-noise ratio of TIC of the expected product [green S/N > 10, amber S/N 1–10]. As an illustration, esculin (7-O-glucopyranosyl esculetin) formation from esculetin* ***31*** *is highlighted, and the representative MS spectrum shows a peak at 339 [M−H$^+$]$^-$, which indicates the formation of the expected product with S/N > 10.*

Donor screening allowed the identification of some unusual and even non-natural donor substrates for UGT72B1, including UDP5SGlc[56] and UDPMan. Indeed, the breadth of donor specificity observed for UGT72B1 was striking compared to the typically highly stringent substrate demands of most GTs and apparently dependent on the nucleotide portion of the donor. Various sugar moieties were tolerated (G or A levels in the screen) for the UDP-donors (UDP-Glc, -5SGlc, -Man, -Gal, -GlcNAc) while the GDP-donors (GDP-Fuc, -Man) were not at all tolerated (Figure 7). This suggests that, for certain GTs, such as UGT72B1, the nucleotide might act as a specificity-determining "tag" for the sugar. This in turn suggests that synthesis of non-natural analogues with the correct nucleotide "tag" could be a possible strategy for the introduction of different sugars by

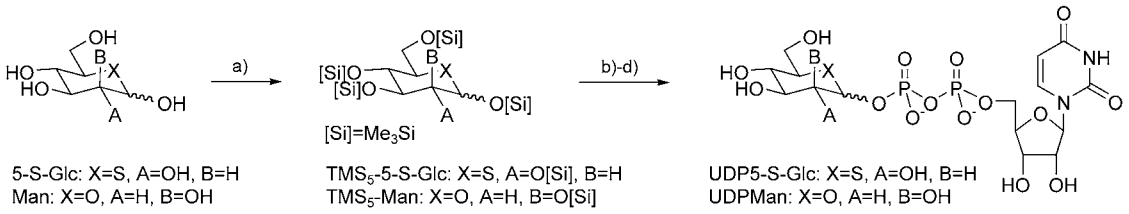

Scheme 6. *The synthesis of UDP-Man and UDP-5SGlc according to the method of Hindsgaul et al.[55] a) Me_3SiCl, pyr, −78 °C; b) Me_3SiI, CH_2Cl_2, −78 °C; c) Bu_4NUDP then Bu_4NF; d) alkaline phosphatase, Tris buffer pH 7.4. Overall yield: 8% UDPMan; 12% UDP5SGlc.*

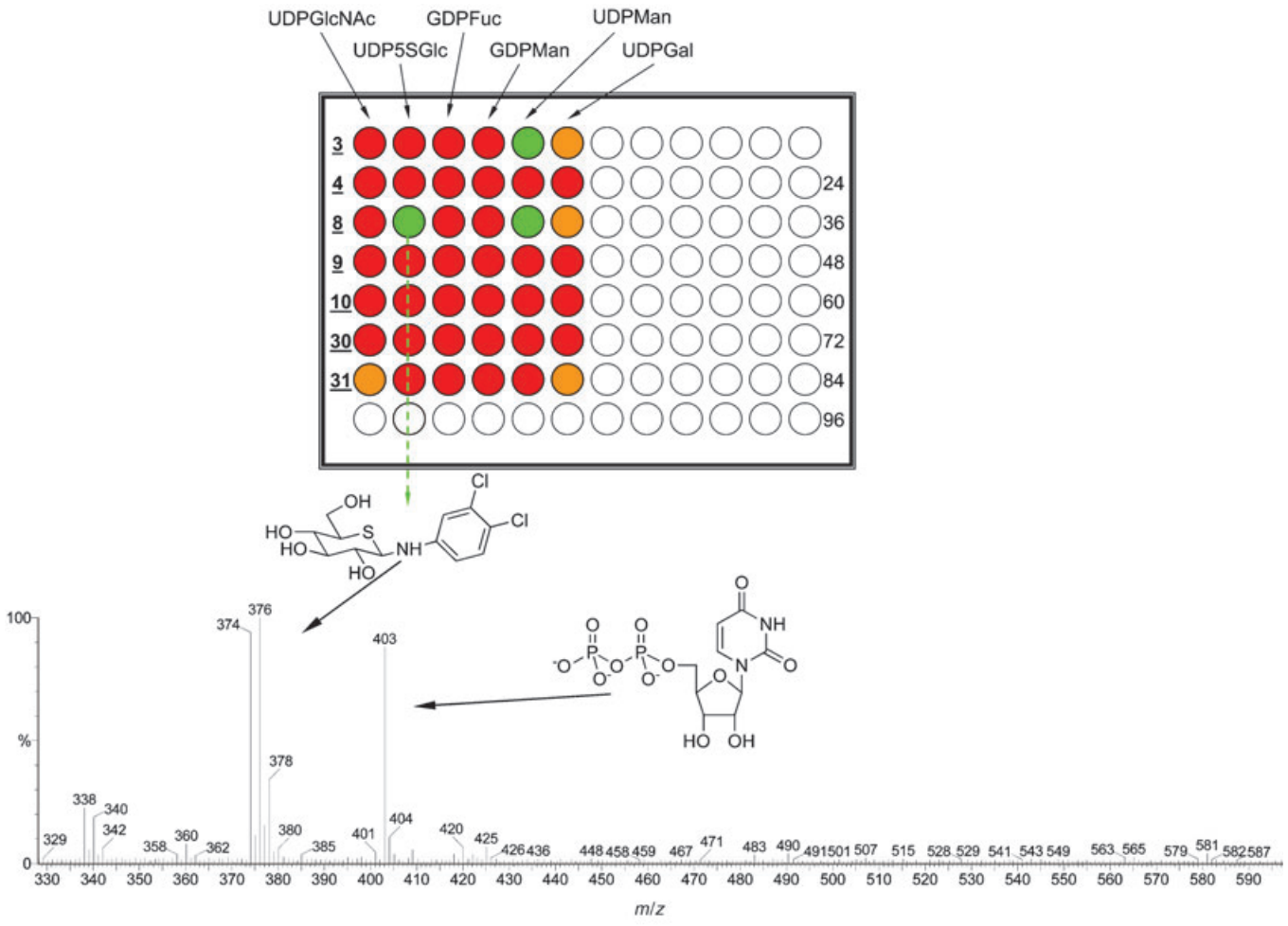

Figure 7. *Mass spectroscopic screening by using the GAR system for activity of UGT72B1 towards a mixed panel of acceptor and donor substrates. As an illustration, the highlighted result shows the corresponding spectrum for the previously unknown UGT72B1-catalysed reaction of α-UDP5SG with 3,4-DCA.*

using Gly-Ts on the path to the goal of "glycorandomisation".[57–65] Interestingly, these results also parallel broad donor sugar-moiety plasticity observed for powerful transferase inhibitors in which the donor sugar moiety was successfully replaced by aromatic groups.[66,67]

Conclusion

ESI-MS provides an excellent method for monitoring multisubstrate enzymes, especially where the substrates and products do not have distinct chromo- or fluorophoric absorptions or emissions. A novel HTS-MS method has allowed full kinetic parameters for multisubstrate enzymes to be determined by using the rapid-equilibrium assumption model. Kinetic parameters for two very different GTs match well with those reported previously, and we propose that the GT mechanism (ordered or random bi bi) is dependent upon the ratio between K_A and K_B with ratios >10 diagnostic of ordered bi bi and ratios <10 seen to be random bi bi. By this rule of thumb, both β-GalT and UGT72B1 follow random bi bi mechanisms, with acceptors slightly preferred over donors with respect to binding affinities. An HTS green-amber-red (GAR) broad screening method has

also been developed as a fast and reliable way of finding potential acceptors and donors, and has been used here to highlight a plasticity in the substrate tolerance of the recently isolated GT, UGT72B1.[14] This useful HTS MS method will now be extended to determining the kinetic parameters with a wider range of donors and acceptors by using a diversity of GTs cloned from microbes, plants and animals.

Experimental Section

General experimental: α-UDP-D-glucose (UDPGlc), α-UDP-D-GlcNAc (UDPGlcNAc), GDP-L-fucose (GDPFuc), GDP and other chemicals were purchased from Sigma, as was bovine β-1,4 galactosyltransferase (βGalT-milk). Recombinant β-1,4-galactosyltransferase (rβGalT) was purchased from Calbiochem. BL21-DE3 rosetta was purchased from Novagen. Sepharose blue was purchase from Amersham. Instruments used: Waters ZMD-MS (ESI^-), Waters 600 HPLC system with Waters 2700 sampler. The MS was operated by Micromass MassLynx 3.3, and the data were processed by using MassLynx 3.5, Microsoft Excel 2002 and Origin 7.

Enzyme expression and purification: *E. coli* BL21-DE3 rosetta were transformed with a UGT72B1-encoding plasmid in a pET-11d vector, cultured and induced by using IPTG as described previously.[15] Cells were then harvested by centrifugation (9 k, 4 °C, 25 min) and sonicated in Tris buffer (7 mL, 20 mM, pH 7.8 containing 1 mM 1,4-dithiothreitol (DTT); Buffer A) prior to recentrifugation and application of the supernatant onto a Sepharose blue column (5 mL). After washing with buffer A at 1 mL min^{-1} for 2 h until all nonbinding proteins had been eluted, the column was eluted with buffer A containing 1 mM UDPGlc. Fractions were collected every 5 mL, and activities were tested by MS. Active fractions were dialysed and freeze-dried, and the purities of proteins analysed by 12.5% SDS-PAGE. Enriched fractions were combined together and dissolved in deionised water, and the solution was loaded onto an anion-exchange column (MONO-Q) and eluted by using a linear gradient (mobile phase A: buffer A, mobile phase B: buffer A containing 250 mM NaCl; method: 100% A for 10 min, 100% A–100% B over 50 min, 100% B for 60 min, 100% A for 120 min; flow rate: 1 mL min^{-1}; detector: UV 280 nm). The resulting GT solution was stored at 4 °C.

MS kinetic-parameter determination

General methods: A Waters ZMD-MS with electrospray ionisation operating in negative mode (ESI^-) was interfaced with a Waters 600 HPLC system and Waters 2700 sampler. MS analysis was under the control of Micromass Masslynx 3.3 software, and data were processed with Masslynx 3.5, Microsoft Excel 2002 and Origin 7. The HPLC/auto-sampler control was divided into two stages: a) injection with the internal standard (0.1 mM; conditions: mobile phase: ACN/H_2O 50:50; flow rate: 0.12 mL min^{-1}; isocratic method for 0.1 min; injection volume: 10.0 μL; syringe rinse: 50 μL, speed setting: 1; loop rinse: 200 μL, speed setting 1; ion type: electrospray negative; 150–1000 ESI^- for 0.1 min, scan 0.2 min) and b) sample injection (conditions: mobile phase: ACN/H_2O 50:50; flow rate: 0.12 mL min^{-1}; isocratic method for 5.5 min; injection volume: 10.0 μL; syringe rinse: 200 μL, speed setting: 16; Loop rinse: 200 μL, speed setting 16; ion type: electrospray negative; ESI^- (single-ion monitoring) for 5.3 min; single-ion peaks monitored, typically: UDPGlc (565.0, dwell 0.1 s), acceptor ($[M+^{35}Cl^-]^-$, UDP (403.0, dwell 0.1 s), GDP (442.0, dwell 0.1 s), product ($[M+^{35}Cl^-]^-$, dwell 0.1 s)]

Typical procedure for standard-curve determination: All reactions were performed in TRIS buffer (1 mM, pH 7.8, containing appropriate cofactors) at ambient temperature. Six samples were analysed with one containing 0.1 mM GDP (in TRIS buffer) only, and the other five containing fixed concentrations of UDPGlc (0.01 mM, 0.03 mM, 0.05 mM, 0.07 mM, 0.09 mM), acceptor (same concentrations as donor), UDP (0.001 mM, 0.003 mM, 0.005 mM, 0.007 mM, 0.009 mM, respectively), product (same as UDP). Injection of GDP internal standard was immediately followed by injection of the standard mixture (10 μL). The peak area was measured for each compound after normalisation for ionisation efficiency by using the internal standard. Plots were drawn of the ratio (X/GDP) against concentration, and the slope was used to obtain concentration information during subsequent reactions.

Typical procedure for kinetic-parameter determination: Six vials were prepared, one containing GDP (0.1 mM), the other five containing fixed concentrations of acceptor with varying concentration of the donor UDPGlc (20 μM, 40 μM, 60 μM, 80 μM and 100 μM). Each batch of substrates was then made up to a total volume to 300 μL with the 1 mM Tris reaction buffer. Initial screening of samples was performed before any enzyme addition, by following the same two-stage procedure described above. After enzyme addition (10 μL into final volume 300 μL), the reaction was monitored every 5.5 min ×16. After each injection, TIC was monitored for all compounds where possible (e.g., 3,4-DCA was below mass limits). This procedure was then used with the concentration of acceptor at 20, 60 and 100 μM. Nonlinear regression was performed by using Origin 7 with typical $R^2 > 0.93$ at 95% confidence. Regression with point data (five points each line) gave almost the same K_M and K_I, but with the larger errors that are a function of the alternative regression method used. For UGT72B1 (M_W 52 928 Da) the reaction buffer was Tris (1 mM, pH 7.8, containing 1 mM DTT) and $[E]_0 \sim 1–5\times10^{-10}$ M.

For β-GalT (M_W 48 500[68]) the reaction buffer was Tris (1 mM, pH 7.8, containing 0.1 mM $MnCl_2$) and $[E]_0 \sim 0.5–2\times10^{-8}$ M.

Comparison of β-GalT activities: A single concentration initial-rate determination was performed by using the standard parameter-determination conditions with UDPGal (500 μM) and MUGlcNAc (500 μM) in Tris buffer (1 mM, $MnCl_2$ 0.1 mM) with identical concentrations (1×10^{-8} M) of bovine β-GalT purified from milk (βGalT-milk) and recombinant β-GalT (rβGalT).

MS GAR screening for GT activity: For UGT72B1, each well in the 96-well plate contained Tris buffer (1.0 mM, pH 7.8, 100 μL), donor (10 mM, 5 μL), acceptor (10 mM, 5 μL) and enzyme (1 mg mL^{-1}, 5 μL). For β-GalT, each well in the 96-well plate contained Tris buffer (1.0 mM, pH 7.8, with 0.1 mM $MnCl_2$, 100 μL), donor (10 mM, 5 μL), acceptor (10 mM, 5 μL) and enzyme (0.35 mg mL^{-1}, 5 μL). For both enzymes, the plates were incubated at 37 °C for timed intervals (up to 8 h), and the presence of products was monitored by MS (full scan from 150–1100 Da). The S/N ratio of product to background was used as a qualitative "green-amber-red" guide of activity (S/N > 10 → green; S/N = 1–10 → amber). In all cases, control solutions without enzyme were used to determine the presence of any uncatalysed background reaction.

Enzyme-catalysed synthesis of *N*-D-β-glucopyranosyl-3,4-dichloroaniline: Solutions of α-UDPglucose (10 mM, 2 mL), 3,4-dichloroaniline (10 mM, 2 mL) and UGT72B1 (1 mg mL^{-1}, 50 μL) in Tris buffer (20 mM, pH 7.8) were combined and diluted with a further 20 mL of buffer and incubated at 37 °C. After 16 h, MS indicated the complete conversion of starting materials, and the reaction was quenched by heating it at 80 °C for 10 min. Dowex 1 (2 g) was

added to the solution, which was then stirred for 1 h. After filtration, the solution was freeze dried, redissolved in deionised water (1 mL), purified by BioGel-P2 Gel column chromatography (25× 400 mm, flow rate: 1 mL min^{-1}, deionised water, UV detection 254 nm, $t=2.4$ h) and freeze dried to obtain the title product as a white solid (4.6 mg, 68%). ^{1}H NMR (400 MHz; D_2O): $\delta=3.32$ (dd, $J=9.3$, 9.1 Hz, 1H; H_2), 3.46 (m, 1H; H_5), 3.48 (t, $J=9.4$ Hz, 1H; H_3), 3.60 (dd, $J=5.3$, 7.1 Hz, 1H; H_6), 3.78 (dd, $J=2.3$, 10.2 Hz, 1H; H_6'), 4.5 (d, $J=8.8$ Hz, 1H; H_1), 6.68 (dd, $J=2.5$, 6.3 Hz, 1H; H_6 in Ph), 6.90 (d, $J=2.2$ Hz, 1H; H_5 in Ph), 7.25 (d, $J=8.9$ Hz, 1H; H_2 in Ph); HRMS *m/z* (ESI$^-$): 357.9983 [M+Cl$^-$]$^-$, (calcd 358.0016); HRMS *m/z* (CI$^+$): 341.0692, [M+NH_4^+]$^+$, (calcd 341.0671).

Synthesis of α,β-D-UDPMannose: D-Mannose (505 mg, 2.81 mmol) was dissolved in anhydrous pyridine (15 mL), and the solution was cooled to 0 °C. Chlorotrimethylsilane (3.0 mL, 20 mmol) was added dropwise, and the resulting solution was stirred for 10 min and then taken to room temperature and stirred for a further 1 h. The formation of a white solid (pyridinium hydrochloride) was observed. After 1 h, the solvent was removed in vacuo. The residue was partitioned between pentane (30 mL) and deionised water (1 mL). The organic fraction was washed with deionised water (5× 1 mL), dried (anhydrous Na_2SO_4) and filtered, and the solvent was removed in vacuo to give a colourless syrup (1.364 g, 95%) that was shown by crude ^{1}H NMR to contain predominately the β-anomer of persilylated mannose. ^{1}H NMR (400 MHz; $CDCl_3$) $\delta=0.11$ (s, 9H; $(CH_3)_3$Si-), 0.12 (s, 9H; $(CH_3)_3$Si-), 0.17 (s, 9H; $(CH_3)_3$Si-), 0.18 (s, 9H; $(CH_3)_3$Si-), 0.19 (s, 9H; $(CH_3)_3$Si-), 3.58 (m, 1H; H_5), 3.62 (t, $J=$ 2.1 Hz, 1H; H_2), 3.70 (dd, $J=6.2$, 7.2 Hz, 2H; H_6, H_4); 3.82 (dd, $J=$ 2.6, 4.6 Hz, 2H; H_3, H_6'); 4.88 (d, $J=2.3$ Hz, 1H; H_1); ^{13}C NMR (100 MHz; $CDCl_3$) $\delta=-0.18$ ($(CH_3)_3$Si-), −0.02 ($(CH_3)_3$Si-), 0.4 ($(CH_3)_3$Si-), 0.6 ($(CH_3)_3$Si-), 0.65 ($(CH_3)_3$Si-), 62.5 (C_6), 68.2 (C_3), 72.0 (C_4), 74.4 (C_5), 75.2 (C_2), 95.6 (C_1); *m/z* (ES$^+$): 563.2 [M+Na^+]$^+$ (ES$^+$). The crude mixture was used without further purification.

UDP disodium salt (200 mg, 0.45 mmol) was dissolved in deionised water (10 mL), and the solution was passed through a Dowex 50W-X8 (H) column (15×30 mm). The pH of the eluent was adjusted to 6.7 with 40% tetra-*n*-butylammonium hydroxide solution. After the solution had been freeze-dried, the desired product was obtained as a white solid (400 mg, 98%). The product was used directly in the next reaction.

1,2,3,4,6-Penta-*O*-trimethylsilyl-D-mannose (153 mg, 0.30 mmol) was dissolved in anhydrous CH_2Cl_2 (1.5 mL), and iodotrimethylsilane (45 μL, 0.30 mmol) was added slowly to the solution at −78 °C. The reaction system was stirred for 30 min and taken to room temperature. A solution of nBu$_4$NUDP (from 120 mg UDP, 0.3 mmol, in 6 mL dry CH_2Cl_2) was then added, and the solution was stirred for a further 4 h. A solution of nBu$_4$NF (1 M in THF, 0.6 mL) was added to the mixture, and the mixture was stirred for a further 1 h. The solvent was removed in vacuo to give the crude product as a light brown solid. The residue was dissolved in Tris buffer (50 mM, pH 7.4, 20 mL), alkaline phosphatase (150 units) was added, and the resulting solution was stirred for 16 h at room temperature. The solution was freeze dried and redissolved in deionised water (4 mL), filtered (0.8 μM filter), purified by reversed-phase (C18) HPLC (0.2 mL×20 samples) isocratic method with ACN/nBu$_4$NBr (0.1% aq.) 30:70, retention time = 12.5 min and Bio-Gel-P2 Gel column chromatography (1.1 g loaded in 3 mL, eluted with deionised water at 1 mL min^{-1}, retention time = 60 min) and freeze-dried to give α,β-UDPMan (13 mg, 8% overall, $\alpha/\beta=5:3$) as a white solid. ^{1}H NMR (400 MHz, D_2O): $\delta=3.31$ (dd, $J=1.8$, 4.8 Hz, 1H; H_6, β), 3.42 (m, 1H; H_6', β), 3.44 (t, $J=9.4$ Hz, 1H; H_4, β), 3.51 (t, $J=10.1$ Hz, 1H; H_6, α), 3.55 (m, 1H; H_5, β), 3.60 (m, 1H, H_3, β), 3.62 (m, 2H; H_4, α, H_6', α), 3.74 (m, 1H; H_5, α), 3.81 (dd, $J=3.3$, 6.3 Hz, 1H; H_3, α), 3.9 (dd, $J=1.5$, 1.7 Hz, 1H; H_2, α), 3.98 (d, $J=3.0$ Hz, 1H; H_2, β), 4.08 (m, 2H; $H_{5,5'}$ (F), α and β), 4.11 (m, 1H; H_4, (F), α,β), 4.2 (m, 1H; H_3 (F), α,β), 4.3 (dd, $J=1.9$, 2.0 Hz, 1H; H_2 (F), α and β), 5.1 (d, $J=8.8$ Hz, 1H; H_1, β), 5.4 (d, $J=7.1$ Hz, 1H; H_1', α), 5.84 (d, 1H; H_1 (F), α, β), 5.86 (d, 1H; H (U), β), 7.82 (d, $J=8.0$ Hz, 1H; H_a (U), β), 7.84 (d, $J=8.0$ Hz, 1H; H_b, α); ^{31}P NMR (166 MHz; D_2O): $\delta=$ −10.5 (2P, α,β), −12.5 (2P, α,β); HRMS *m/z* (EI$^-$): 565.0469, [M−H$^+$]$^-$, (calcd 565.0472).

Synthesis of α,β-D-UDP-5-thio-glucose: 5-Thio-D-glucopyranose (100 mg, 0.51 mmol) was dissolved in anhydrous pyridine (2 mL), and the solution was cooled to 0 °C in an ice bath. Chlorotrimethylsilane (0.6 mL, 4.1 mmol) was added dropwise to the reaction mixture, and the solution was stirred for a further 1 h at room temperature. The formation of a white solid (pyridinium hydrochloride) was observed. The solvent was removed, and the residue was partitioned between hexane (20 mL) and deionised water (1 mL). The hexane fraction was washed (deionised water 5×1 mL), dried (anhydrous Na_2SO_4) and filtered, and the solvent was removed to give crude TMS$_5$5-S-Glc as a colourless syrup (α/β 95:5, 277 mg, 98%). ^{1}H NMR (400 MHz; $CDCl_3$): $\delta=0.13$ (s, 9H; $(CH_3)_3$Si-), 0.15 (s, 9H; $(CH_3)_3$Si-), 0.16 (s, 9H; $(CH_3)_3$Si-), 0.17 (s, 9H; $(CH_3)_3$Si-), 0.20 (s, 9H; $(CH_3)_3$Si-), 3.20 (m, 1H; H_5), 3.61 (1H; m, H_6), 3.59 (dd, $J=6$, 8 Hz, 1H; H_3); 3.64 (dd, $J=9$, 10 Hz, 1H; H_4); 3.72 (dd, $J=2.5$, 5 Hz, 1H, H_2); 3.88 (m, 1H; H_6'); 4.74 (d, $J=2.3$ Hz, 1H; H_1); *m/z* (EI) 579.1 [M+Na$^+$] (ES$^+$)

The crude mixture was used without further purification.

1,2,3,4,6-Penta-*O*-trimethylsilane-5-thio-D-glucopyranose (277 mg, 0.50 mmol) was dissolved in anhydrous CH_2Cl_2 (3 mL), and iodotrimethylsilane (72 μL, 0.50 mmol) was added slowly to the resulting solution. The reaction system was stirred at room temperature for 30 min. nBu$_4$NUDP (380 mg, 0.42 mmol) was then added, and the solution was stirred for a further 4 h. After 4 h, nBu$_4$NF (1 M in THF, 1.1 mL) was added to the mixture, which was stirred for a further 1 h. After 1 h, the organic solvent was removed under vacuum to give the crude product as a light brown solid. The residue was dissolved in Tris buffer (50 mM, pH 7.4, 30 mL), alkaline phosphatase (200 units) was added, and the resulting solution was stirred for 16 h at room temperature. The solution was freeze dried and redissolved in deionised water (4 mL), filtered (0.8 μM filter), purified by reversed-phase (C18) HPLC (0.5 mL×20 samples, isocratic method with1 ACN/nBu$_4$NBr (0.1% aq.) 30:70, retention time = 19.4 min) and Bio-Gel-P2 Gel column chromatography (700 mg loaded in 5 mL, eluted with deionised water at 1 mL min^{-1}, retention time = 180 min) and freeze-dried to give UDP-5S-Glc as a white solid (40 mg, 12%, α/β 3:7). ^{1}H NMR (400 MHz, D_2O): $\delta=0.821$ (t, $J=$ 7.4 Hz, 12H; 4CH_3CH$_2$CH$_2$CH$_2$-, α), 0.825 (t, $J=7.3$ Hz, 12H; 4CH_3CH$_2$CH$_2$CH$_2$-, β), 1.19 (q, $J=7.4$ Hz, 8H; 4CH$_3$$CH_2CH_2CH_2$-, α), 1.19 (q, $J=7.4$ Hz, 8H; 4CH$_3$$CH_2CH_2CH_2$-, β), 1.42 (m, 8H; 4CH$_3CH_2$$CH_2CH_2$-, α), 1.42 (8H; m, 4CH$_3CH_2$$CH_2CH_2$-, β), 2.86 (m, 1H; H_5, β), 3.08 (t, $J=8.2$, 9.5 Hz, 8H; 4CH$_3$CH$_2$CH$_2$$CH_2$-, α), 3.08 (t, $J=8.2$, 9.5 Hz, 8H; 4CH$_3$CH$_2$CH$_2$$CH_2$-, β), 3.19 (m, 1H; H_5, α), 3.20 (t, $J=10$ Hz, 1H; H_3, β), 3.43 (t, $J=10$ Hz, 1H; H_4, α), 3.43 (t, $J=10$ Hz, 1H; H_4, β), 3.50 (m, 1H; H_3, α), 3.50 (m, 1H; H_6', α), 3.51 (m, 1H; H_6, α), 3.52 (q, $J=3.5$ Hz, 1H; H_2, β), 3.60 (m, 1H; H_2, α), 3.80 (m, 1H; H_6', β), 3.80 (m, 1H; H_6, β), 4.15 (m, 3H, H_2, H_3, H_4 (F), α), 4.15 (m, 3H; H_2, H_3, H_4 (F), β), 4.20 (m, 2H; H_5 and $H_{5'}$ (F), α), 4.20 (m, 2H; H_5, $H_{5'}$ (F), β), 5.01 (t, $J=8.8$ Hz, 1H; H_1, β), 5.26 (q, $J=2.4$, 5.6 Hz, 1H; H_1, α), 5.85 (m, 2H; H_b, H_1(F)), α), 5.85 (m, 2H; H_b, H_1 (F), β), 7.82 (d, $J=9$ Hz, 1H; H_a, α), 7.82 (d, $J=9$ Hz, 1H; H_a, β); ^{31}P NMR (166 MHz; D_2O; HDO) $\delta=-10.50$ (d, $J=20.3$, 1P; α), −12.09 (q, $J=$

17.84 Hz, 1P; α), −10.50 (d, J = 20.3 Hz, 1P; β), −11.92 (q, J = 8.6, 20.74 Hz, 1P; β); m/z (EI) 822.16, $[M+nBu_4N^+-2H^+]^-$ (ES^-)

Acknowledgements

This research was funded by the BBSRC under the Exploiting Genomics Initiative (BBSRC 87/EGA16205). We would like to thank Drs Neil Oldham and Jo Kirkpatrick for providing technical advice on MS.

Keywords: enzymes · glycosyltransferases · high-throughput screening · kinetics · mass spectrometry

[1] L. F. Leloir, *Science* **1971**, *172*, 1299.
[2] P. M. Coutinho, B. Henrissat, AFMB-CNRS Carbohydrate-Active Enzymes server: http://afmb.cnrs-mrs.fr/CAZY, *Vol. 2003*, **1999**.
[3] M. M. Palcic, K. Sujino, *Trends Glycosci. Glycotechnol.* **2001**, *13*, 361.
[4] M. M. Palcic, M. Pierce, O. Hindsgaul, *Methods Enzymol.* **1994**, *247*, 215.
[5] M. F. Verostek, R. B. Trimble, *Glycobiology* **1995**, *5*, 671.
[6] C. L. M. Stults, B. J. Wilbur, B. A. Macher, *Anal. Biochem.* **1988**, *174*, 151.
[7] S. C. Crawley, O. Hindsgaul, G. Alton, M. Pierce, M. M. Palcic, *Anal. Biochem.* **1990**, *185*, 112.
[8] D. K. Fitzgerald, B. Colvin, R. Mawal, K. E. Ebner, *Anal. Biochem.* **1970**, *220*, 92.
[9] N. Taniguchi, A. Nishikawa, S. Fujii, J. Gu, *Methods Enzymol.* **1989**, *179*, 397.
[10] H. Gao, J. A. Leary, *J. Am. Soc. Mass. Spectrom.* **2003**, *14*, 173.
[11] A. J. Norris, J. P. Whitelegge, K. F. Faull, T. Toyokuni, *Biochemistry* **2001**, *40*, 3774.
[12] E. D. Lee, W. Muck, J. D. Henion, T. R. Coveys, *J. Am. Chem. Soc.* **1989**, *111*, 4600.
[13] N. Pi, J. A. Leary, *J. Am. Soc. Mass Spectrom.* **2004**, *15*, 233.
[14] As a representative illustration of the relative throughput, the method disclosed here allowed the determination of ~200–300 TICs to create ~15–20 initial rate measurements in only ~1200 min and thus allows sufficiently broad coverage of substrate-concentration variations to allow full bi-bi parameter determination of UGT72B1. This need for sufficient velocity measurements to allow accurate parameter determination has resulted in most kinetic determinations for GTs being conducted under less informative pseudo-single-substrate conditions. By the same token, an entire 96-well plate substrate-screening GAR assay (vide infra) can be conducted in just 300 min.
[15] C. Loutre, D. P. Dixon, M. Brazier, M. Slater, D. J. Cole, R. Edwards, *Plant J.* **2003**, *34*, 485.
[16] Y. Kanie, A. Kirsch, O. Kanie, C. H. Wong, *Anal. Biochem.* **1998**, *263*, 240.
[17] D. Bowles, *Biochem. Soc. Trans.* **2002**, *30*, 301.
[18] P. A. Steenkamp, F. R. van Heerden, B. E. van Wyk, *Forensic Sci. Int.* **2002**, *127*, 208.
[19] L. Michaelis, M. L. Menten, *Biochem. Z.* **1913**, *49*, 333.
[20] G. E. Briggs, J. B. S. Haldane, *Biochem. J.* **1925**, *19*, 338.
[21] P. Roepstorff, *Curr. Opin. Biotechnol.* **1997**, *8*, 6.
[22] S. Ainsworth, *Steady-State Enzyme Kinetics*, MacMillan, London, **1977**.
[23] E. L. King, C. Altman, *J. Phys. Chem.* **1956**, *60*, 1375.
[24] W. W. Cleland, *Biochim. Biophys. Acta* **1963**, *67*, 104.
[25] D. V. Roberts, *Enzyme Kinetics*, Cambridge University Press, New York, **1977**.
[26] R. O. Hurst, *Can. J. Biochem.* **1969**, *47*, 941.
[27] M. Dixon, *The Enzymes*, LongMans Green and Co., New York, **1958**.
[28] U. M. Unligil, S. Zhou, S. Yuwaraj, M. Sarkar, H. Schachter, J. M. Rini, *EMBO J.* **2000**, *19*, 5269.
[29] G. Schmid, H. Grisebach, *Eur. J. Biochem.* **1982**, *123*, 363.
[30] A. E. Kearns, S. C. Campbell, J. Westley, N. B. Schwartz, *Biochemistry* **1991**, *30*, 7477.
[31] L. Chen, H. Men, S. Ha, X.-Y. Ye, L. Brunner, Y. Hu, S. Walker, *Biochemistry* **2002**, *41*, 6824.
[32] P. Louisot, P. Belon, P. Broquet, *C. R. Seances Acad. Sci. Ser. D* **1976**, *283*, 401.
[33] E. Bause, G. Legler, *Biochem. J.* **1981**, *195*, 639.
[34] J. Rini, U. M. Unligil, H. Schachter, *PCT Int. Appl.* WO2000078936, **2000**, 307pp.
[35] L. M. Quiros, J. A. Salas, *J. Biol. Chem.* **1995**, *270*, 18234.
[36] L. M. Quiros, R. J. Carbajo, J. A. Salas, *FEBS Lett.* **2000**, *476*, 186.
[37] J. L. Kadrmas, C. R. Raetz, *J. Biol. Chem.* **1998**, *273*, 2799.
[38] T. Garcia, N. Sanchez, M. Martinez, J. Aracil, *Enzyme Microb. Technol.* **1999**, *25*, 584.
[39] T. Ohshima, Y. Ito, H. Sakuraba, S. Goda, Y. Kawarabayasi, *J. Mol. Catal. B* **2003**, *23*, 281.
[40] G. D. Yadav, K. M. Devi, *Biochem. Eng. J.* **2002**, *10*, 93.
[41] J.-S. Han, Y. Kosugi, S. Ando, H. Ishida, K. Ishikawa, *Jpn. Kokai Tokkyo Koho* **2002**, 12pp.
[42] J.-M. Mouillon, S. Ravanel, R. Douce, F. Rebeille, *Biochem. J.* **2002**, *363*, 313.
[43] J. Attieh, S. A. Sparace, H. S. Saini, *Arch. Biochem. Biophys.* **2000**, *380*, 257.
[44] E. Rajashekhara, M. Kitaoka, Y.-K. Kim, K. Hayashi, *Biosci. Biotechnol. Biochem.* **2002**, *66*, 2578.
[45] X. R. Sheng, X. Li, X. M. Pan, *J. Biol. Chem.* **1999**, *274*, 22238.
[46] D. C. Lamb, A. G. S. Warrilow, K. Venkateswarlu, D. E. Kelly, S. L. Kelly, *Biochem. Biophys. Res. Commun.* **2001**, *286*, 48.
[47] H. Wu, Y. Zheng, Z.-X. Wang, *Biochemistry* **2003**, *42*, 1129.
[48] Z. Lai, K. V. Ferry, M. A. Diamond, K. E. Wee, Y. B. Kim, J. Ma, T. Yang, P. A. Benfield, R. A. Copeland, K. R. Auger, *J. Biol. Chem.* **2001**, *276*, 31357.
[49] J. Y. Chou, M. F. Singer, P. McPhie, *J. Biol. Chem.* **1975**, *250*, 508.
[50] C. H. Wong, G. M. Whitesides, *Enzymes in Synthetic Organic Chemistry*, Pergamon, Oxford, **1990**.
[51] J. F. Morrison, K. E. Ebner, *J. Biol. Chem.* **1971**, *246*, 3985.
[52] J. E. Bell, T. A. Beyer, R. L. Hill, *J. Biol. Chem.* **1976**, *251*, 3003.
[53] B. Ramakrishnan, P. S. Shah, P. K. Qasba, *J. Biol. Chem.* **2001**, *276*, 37665.
[54] See Supporting Information.
[55] T. Uchiyama, O. Hindsgaul, *J. Carbohydr. Chem.* **1998**, *17*, 1181.
[56] M. Yang, PhD thesis, University of Huddersfield (UK), **2003**.
[57] C. Albermann, A. Soriano, J. Jiang, H. Vollmer, J. B. Biggins, W. A. Barton, J. Lesniak, D. B. Nikolov, J. S. Thorson, *Org. Lett.* **2003**, *5*, 933.
[58] W. A. Barton, J. B. Biggins, J. Jiang, J. S. Thorson, D. B. Nikolov, *Proc. Natl. Acad. Sci. USA* **2002**, *99*, 13397.
[59] W. A. Barton, PhD thesis, Cornell University (USA) **2002**.
[60] W. A. Barton, J. Lesniak, J. B. Biggins, P. D. Jeffrey, J. Jiang, K. R. Rajashankar, J. S. Thorson, D. B. Nikolov, *Nat. Struct. Biol.* **2001**, *8*, 545.
[61] C.-W. T. Chang, B. Elchert, Y. Hui, J. Li, J. Wang, R. Rai, J. Takemoto, *Abstracts of Papers, 226th ACS National Meeting, New York, NY, United States, September 7–11, 2003* **2003**, CARB.
[62] X. Fu, C. Albermann, J. Jiang, J. Liao, C. Zhang, J. S. Thorson, *Nat. Biotechnol.* **2003**, *21*, 1467.
[63] D. Hoffmeister, J. Yang, L. Liu, J. S. Thorson, *Proc. Natl. Acad. Sci. USA* **2003**, *100*, 13184.
[64] J. S. Thorson, J. Jiang, W. A. Barton, J. B. Biggins, J. Lesniak, D. B. Nikolov, *Abstracts of Papers, 221st American Chemical Society National Meeting*, San Diego (USA), **2001**.
[65] J. Yang, X. Fu, Q. Jia, J. Shen, J. B. Biggins, J. Jiang, J. Zhao, J. J. Schmidt, P. G. Wang, J. S. Thorson, *Org. Lett.* **2003**, *5*, 2223.
[66] B. Muller, C. Schaub, R. R. Schmidt, *Angew. Chem.* **1998**, *110*, 3021; *Angew. Chem. Int. Ed.* **1998**, *37*, 2893.
[67] A. K. Bhattacharya, F. Stolz, R. R. Schmidt, *Tetrahedron Lett.* **2001**, *42*, 5393.
[68] S. C. Magee, R. Mawal, K. E. Ebner, *J. Biol. Chem.* **1973**, *248*, 7565.

Received: April 9, 2004
Revised: September 7, 2004

